Frequency Domain Spectroscopy Measurements of Oil-paper Insulation for Energized Transformers

Xu Yang, Shawn Nielsen and **Gerard Ledwich**
School of Electrical Engineering and Computer Science
Queensland University of Technology
2 George Street, Brisbane QLD 4000, Australia

ABSTRACT

Frequency Domain Spectroscopy (FDS) is proposed as a suitable diagnostic method in this paper for implementation on energized oil-paper insulation systems. In present FDS tests, the measurement method is only designed for offline applications. To overcome the deficiencies with the offline testing, this work investigates the feasibility of performing FDS measurements on energized transformers with the view to developing an online diagnostic tool using neutral connections as injection and measurement paths. In the proposed technique, a low-pass filter system is designed to remove the high frequency noise as well as the power frequency signals present in the measured neutral currents. The technique has been successfully applied in a laboratory environment on transformers with oil-paper insulation systems with different operational ages and is feasible for single-phase as well as 3-phase transformers with the accessible neutral points. Compared with the conventional FDS results, a nonlinear dielectric phenomenon is observed from the energized insulation systems as higher dissipation factor Tanδ values primarily due to the increased losses under power frequency voltage excitation. The degree of the nonlinearity is found to correlate well with the degradation status of insulation systems under test.

Index Terms — **Frequency Domain Spectroscopy, energized power transformer, oil-paper insulation system, nonlinearity, dissipation factor, neutral connections.**

1 INTRODUCTION

DIELECTRIC response measurements are a well-known and widely acceptable technique for the condition diagnosis of oil-paper insulation systems with the advantage of retaining the integrity of insulation system rather than sampling the insulating materials [1-3]. The measurement methods are classified into time and frequency domain techniques [4, 5]. Time domain methods include Return Voltage Measurements (RVM) [3, 6] and Polarization and Depolarization Current (PDC) [7, 8] measurements, while frequency domain methods refer to Frequency Domain Spectroscopy (FDS) [9] measurements. The basic interpretation of the dielectric response results relating to insulation degradation levels has been established and verified in recent decades. However, these measurements so far are only limited to offline applications.

For the large power transformers, offline dielectric response measurements require the unit shutdown and disconnected from the power system for a period, even for days. A potential consequence of the shutdown of a unit for testing may make the system more vulnerable to an outage due to a lack of redundancy and reduce the overall reliability of the power system. And the outage costs of a single offline test on a large power transformer can be significant. Moreover, offline measurements are not fully able to reflect the real situation of an oil-paper insulation system since the electric and thermal stresses on the insulation system are significantly different from an energized transformer and those stresses significantly influence the response results [9-11].

Few studies relating to online dielectric response measurements have been identified so far. Therefore, the purpose of this paper is to enhance the existing methods to implement the dielectric response measurements on energized transformers. Compared with time domain measurements, FDS measurements are a more straightforward method of measuring the impedance of the insulation system without the short or open circuit operations. Moreover, the added advantage of the FDS is that the measurements use specific frequency excitation, such as discrete sinusoidal waves instead of a step voltage as in the PDC and RVM measurements. This provides high accuracy to extract the discrete frequency dielectric response [12]. Therefore, the FDS method is selected as the desired method for energized measurements in this paper.

According to the theory of the FDS method [4], the success of the measurement depends on reliable signal injection and the corresponding current measurement. Thus, two challenges emerge in applying the FDS to an energized insulation system: 1) successfully injecting the testing signal onto energized

Manuscript received on 11 February 2016, in final form 19 February 2017, accepted 19 February 2017. Corresponding author: X. Yang.

transformers; 2) successfully extracting the dielectric response results from energized transformers, which may be swamped by noise or absorbed by other components connected to the power system.

Moreover, the implementation of a conventional FDS measurement at very low frequency takes a long time to complete [4]. The measurement lasts for over 10 hours for frequencies down to 10^{-4} Hz [13]. Such a long time period will increase many risks for the proposed FDS tests, such as the potential of external faults occurring on transformers or load variations during the measurement period. These risks may adversely affect the measured dielectric response and thus lead to difficulties in interpretation. It is therefore desirable to reduce the overall measurement time associated with online FDS measurements.

In this paper, the above difficulties were carefully addressed: a neutral injection and measurement system to accomplish dielectric response measurements on single-phase or 3-phase energized transformer oil-paper insulation systems are developed and investigated. Further, transformers with different operational ages were selected as test objects for affording interpretation of dielectric responses under an energized condition. In addition, special cautions were mentioned in references to keep the field strength lower than 10 V/mm (voltage below 500 V) to avoid nonlinear responses occurring in the dielectric response measurements [14, 15], since nonlinearity of the dielectric response appears if the dielectrics are subjected to an adequately high electric field [16]. Considering the energized condition, the insulation under test is inevitably subjected to a high voltage electric field at power frequency as well as the excitation signal electric field from the FDS tests. Therefore, it is expected that the nonlinear phenomena will be excited from the complex voltage stresses.

2 FREQUENCY DOMAIN SECTROSCOPY MEASUREMENTS

The conventional offline FDS method measures the dissipation factor $\tan\delta(\omega)$ and complex capacitance $C^*(\omega)$ of the insulation system within a frequency band from 10^{-4} Hz to 10^{3} Hz [4]. A sequence of discrete sinusoidal waveforms are injected as an excitation voltage $V_s(\omega)$ onto a de-energized transformer through the shorted HV or LV terminals and the corresponding response current is then measured at the terminals on the another side of the transformer. The response current consists of the "DC conduction component" produced by the movement of the free charges, as well as the displacement current generated by the induced polarization mechanisms [1, 12]. The response current $I_{out}(\omega)$ measured from the insulation system due to an excitation voltage $V_s(\omega)$ is expressed below.

$$I_{out}(\omega) = \mathrm{j}\omega\{C'(\omega) - jC''(\omega)\}V_s(\omega) = \mathrm{j}\omega C^*(\omega)V_s(\omega) = Y^*(\omega)V_s(\omega) \quad (1)$$

here, $C'(\omega)$ is the real part of the complex capacitance $C^*(\omega)$ representing ordinary capacitive response and $C''(\omega)$ is the imaginary part coupled with the losses; $Y^*(\omega)$ is the complex admittance of the insulation system under test; ω is the angular frequency.

Dissipation factor $\tan\delta(\omega)$ as well as complex permittivity $\varepsilon^*(\omega)$ or complex capacitance $C^*(\omega)$ measured from the FDS are the three common indicators used to interpret the deterioration level of the insulation system under test. $\tan\delta(\omega)$ can be expressed as:

$$tan\delta(\omega) = \frac{Y'(\omega)}{Y''(\omega)} = \frac{C''(\omega)}{C'(\omega)} = \frac{\varepsilon''(\omega)}{\varepsilon'(\omega)} \quad (2)$$

Generally, higher values of $\tan\delta(\omega)$ indicate larger degree of aging or degradation in the dielectric [17]. Separation of real and imaginary parts of complex capacitance or permittivity aids in understanding of the capacitive as well as loss components of the insulation system [4].

Attempts to improve the above conventional FDS have been made in recent years, mainly including acceleration of the FDS [18] and investigations on alternative waveforms instead of adopting a series of discrete sinusoidal waveforms as an excitation signal [10]. Koch's technique to accelerate the measurements depends on the combination of time domain polarization current measurements obtaining the low frequency (< 1 Hz) response through Fast Fourier Transform (FFT) with the FDS achieving the high frequency measurements [18]. Jaya in [19] proposes injection of the multiple sinusoidal oscillations with different frequencies simultaneously onto the insulation system under investigation and transfers to frequency domain data through Discrete Fourier Transform (DFT) [20]. In addition, a triangle waveform was utilized in [10] to compare the performance with that of a sinusoidal waveform response and the authors concluded that the estimation of moisture content in paper based on the triangular excitation was more realistic. However, the above improvements were performed under offline conditions associated with relatively low noise levels ensuring reasonable results could be obtained through the FFT processing. Clean results in frequency domain are unattainable if the FFT technique is used to analyze time domain data extracted from within a noisy environment, such as energized measurements. This is primarily due to significant spectrum leakages and/or noise spikes corrupting the measured results [20]. A measurement system called Arbitrary Waveform Impedance Spectroscopy (AWIS) is presented in [21]. This new method can be used to measure the continuous dielectric responses for online applications. However, authors mentioned that AWIS was appropriate for high frequency measurements (>10 Hz). Therefore, these existing efforts are inadequate to solve the issues on the proposed measurements under energized circumstances, especially for low frequency applications.

3 ENHANCEMENTS TO THE FDS MEASUREMENTS

3.1 INJECTION AND MEASUREMENT POINTS

Under energized conditions, the HV and/or LV terminals of the transformer under test are connected with a power network, which are unattainable for the conventional FDS measurements. A mostly possible injection point is through a

bushing tap on the HV side of the transformer utilized in online Frequency Response Analysis (FRA) measurements [22, 23]. However, the coupling path from the bushing tap to the winding is primarily via a low value capacitance. At the low frequencies used during FDS measurements, this will result in a high impedance measurement path. Difficulties with the interpretation of the transformers insulation response will occur if the dielectric responses of the bushings are not separated from the overall measured response.

In this paper, zero or low power frequency potential of transformer windings are utilized as a signal injection point and a response current collection point. Any accessible neutral connections present on the system or transformers under test can satisfy these criteria. The excitation voltage can be directly injected through the accessible neutrals while the measurement of response current primarily relies on a neutral earthing resistor as the current measurement impedance. In terms of 3-phase transformers, the windings can either be formed as a Wye connection or a Delta connection. For Wye-connected windings, an accessible neutral point can be used to inject the excitation $V_s(t)$ or measure the dielectric response voltage $V_{out}(t)$ via an earthing resistor R_n, shown in Figure 1. Since the proposed method relies on neutral connections that are not available for Delta-connected windings, neutral points can be created using suitably connected voltage measurement transformers (VTs), illustrated in Figure 2. The proposed method for single-phase transformers can be applied on the condition that the neutral connections are accessible as well [24]. The expected resistance of R_n for measuring purposes should be in a range from tens to hundreds of ohms to ensure that the response current is measurable to the measuring system. Presently the value of R_n used in this work was chosen to maximize signal to noise ratio. Future work will be done to bring R_n in line with those found in practical systems.

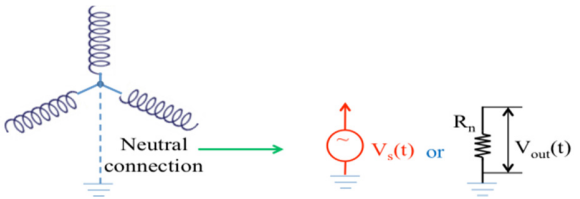

Figure 1. Proposed measurement method for Wye-connected windings.

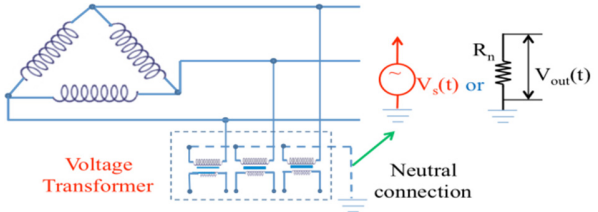

Figure 2. Proposed measurement method for Delta-connected windings.

3.2 DIELECTRIC RESPONSE CURRENT MEASUREMENT

For offline tests, noise is not usually a problem since the apparatus linked with the transformer under test are disconnected with possible noise sources. However, for energized tests, transformers are connected with the grid resulting in the 50Hz neutral current variations in neutral connections due to load fluctuations. In addition to the normal load variation noise, many other sources of noise in substations exist and the majority of them are at high frequencies compared with the low frequency dielectric response, such as, the corona disturbance or harmonics of power frequency. Therefore, the frequency band used in this paper is from 10^{-3} Hz to 10^{0} Hz. instead of high frequencies, which is associated with the moisture content in the solid insulation, pressboard ageing as well as the interfacial polarization [1, 9].

The magnitude of the dielectric response current usually has a range from nA to μA within the low frequency band from 10^{-4} Hz to 1 Hz. To measure these weak signals while reject the high frequency noise, a low-pass filter system is used to extract the low frequency parts of the experimentally measured dielectric response signal. The measurement system consists of two parts. The first part is a passive RC filter designed to attenuate signals at power frequency's and above by ≈90 dB. Figure 3 shows the two parts of the measurement system. This comprises a passive RC filter section and a multi-stage active filter stage with amplification. The active low-pass filter stage is used to further attenuate any signals with frequencies above 1 Hz. The overall amplification in the measurement system is approximately 10^{6}. The active filter is configured as a Butterworth low-pass filter with four stages and a gain of 10^{3} for two stages, illustrated in Figure 3. This filter system is paralleled with the earthing resistor, the designed parameters of which are listed in Table 1. Any variations brought by the filter system will be calibrated out through the calibration method introduced in section 4.1.

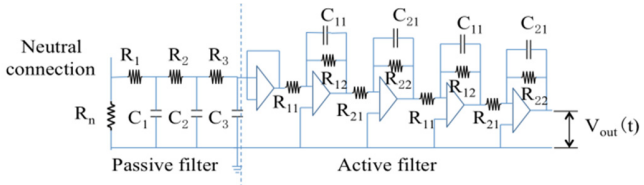

Figure 3. Low-pass filter system

Table 1. Designed Parameters of Low-pass Filter System.

Parameter	Designed values	Parameter	Designed values
R_1	1 kΩ	R_{11}	3.659 kΩ
R_2	10 kΩ	R_{12}	36.587 kΩ
R_3	1000 kΩ	R_{21}	0.3659 kΩ
C_1	100 μF	R_{22}	3 μF
C_2	10 μF	C_{11}	3 μF
C_3	1 μF	C_{21}	3 μF

Considering the other electrical elements in the external network connected to the transformer under test, they may have neutral earthing connections as well, which provide possible split paths for the excitation voltage and the response current. Therefore, the proposed measurement is inevitably confronted with some uncertainties. The uncertainties are mainly influenced by the potential configurations of equipment directly connected with the HV and the LV terminals of the

transformer under test. The possible measurement circuit can be simplified as shown in Figure 4.

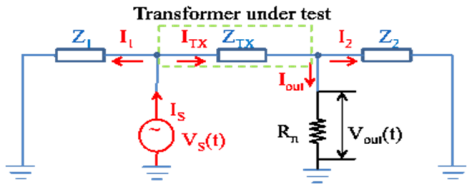

Figure 4. Simplified measurement circuit with external connections.

In Figure 4, the externally connected components that have neutral connections linked with the injection side and measurement side of the transformer under test are modelled as impedance Z_1 and Z_2, respectively, characterized by resistive and capacitive elements for low frequency response. Z_{TX} is the impedance of the insulation system.

For the source side, Z_1 may draw significant current from the signal source if the magnitude of Z_1 is small compared with the insulation impedance Z_{TX}. It is also possible that if this injected current flowing in the external circuitry reaches significant levels, it may cause faults in the network, such as a half-cycle saturation for transformers, which is similar to fault caused by Geomagnetically Induced Current (GIC) [25]. Therefore, it is necessary to consider the magnitude of Z_1 and Z_2 relative to Z_{TX} in ensuring that external currents I_1 and I_2 are safe for the system.

On the measurement side, the dielectric response current I_{TX} is split between the earthing resistor R_n and impedance Z_2 of the external network. In this circumstance, it is desirable that R_n is much smaller than $|Z_2|$, such as $R_n/|Z_2| < 1/10$, so that $9/10$ dielectric current response can be measured. The characteristics of Z_2 are of great importance for phase shift determination. The accurate dielectric current response and transfer function of the insulation system then can be determined; this is given in equation (3) and equation (4), respectively.

$$I_{TX} = I_{out} + \frac{V_{out}}{Z_2} \tag{3}$$

$$Z_{TX} = \frac{V_S}{I_{TX}} \tag{4}$$

Based on the above discussion, the proposed measurement method relies on the availability of suitable connection points for signal injection and extraction. It is also necessary to understand the effects of the externally connected equipment on the injected and measured signals as well as the effects of these signals on the other equipment in the network.

3.3 MEASUREMENTS ACCELERATION

A chirp waveform is proposed as an alternative excitation waveform to address the issue of the duration of tests. The advantage of a chirp excitation is that the signals frequency varies with time and does not need to reach a steady state. Therefore, the duration of the chirp signal is not strictly limited by the lowest frequency as with a discreet sinusoidal signal. The sweep duration of the chirp signal will be primarily determined by the required frequency resolution and analysis requirements of the measurement. The lowest value of the measured response current is typically found at the lowest signal frequency due to the capacitive nature of oil-paper insulation systems. A logarithmic chirp sweep it therefore used, this results in more signal energy in the lower frequency bands. This serves to increase the signal-to-noise ratio of the measured response current in the lower frequency bands. The basic chirp waveform is described in equation (5).

$$V_s(t) = Msin\big(\theta(t)\big) = Msin(2\pi \int f(t)dt) \tag{5}$$

where M is the constant magnitude; $\theta(t)$ represents the instantaneous phase and $f(t)$ is associated with the instantaneous frequency which increases with the time consumed.

The logarithmic frequency sweep rate has an expression shown in equation (6):

$$f(t) = f_0 \times \beta^t \tag{6}$$

where $\beta = (\frac{f_1}{f_0})^{\frac{1}{t1}}$, f_0 is the instantaneous frequency at time 0, and f_1 is the instantaneous frequency at final time t_1.

Consequently, the response current will have a chirp-like waveform coupled with information of an insulation degradation 'fingerprint' expressed as:

$$I_{TX}(t) = B(t)sin\big(2\pi \int f(t)dt + \theta'(t)\big) + n(t) \tag{7}$$

The 'fingerprints' includes the magnitude attenuation $B(t)$, phase shift $\theta'(t)$ coupled with the instant swept frequency and some additive noise $n(t)$ from the measurement.

A chirp-matched filter was designed to perform the task of extracting frequency domain information from a chirp-like waveform signal. This is used instead of using FFT processing due to the non-stationary and nonlinear nature of a chirp signal. More details about the chirp-matched filter can be found in [24].

4 EXPERIMENT RESULTS

Conventional and proposed FDS measurements were done on two SWER (Single Wire Earth Return) transformers as well as a large 3-phase transformer. The details of the tested transformers and voltage measurement transformers are listed in Table 2. Here, 'T1', 'T2' and 'T3' are used to refer to the transformers detailed in the table in all proceeding work.

Table 2. Nameplate Details of The Transformers Under Test.

Terms	T1	T2	T3	VT
Winding configuration	SWER	SWER	Delta-Wye	Single-phase
Manufacture year	1959	2004	2011 (never in service)	--
kVA	5	10	200	0.05

Volts HT /V	12,700	13,900	11,000	11,000
Volts LT /V	250	250	433	110
Manufacture	PWA Electrical Industries	ABB	Wilson	Schneider Electric

4.1 CALIBRATION PROCESS

Calibration is used to account for distortions brought by the measuring system. There are two minor expected distortions in the designed measurement system. One is the magnitude attenuation and phase shift effects of the low-pass filter stage in the measurement chain, particularly when the frequency is close to the filter corner frequency. The second is because of the relatively fast chirp sweep speed at the higher frequencies may not provide the perfect phase responses. The calibration process is to identify the distortions by measuring the response of a large value resistor with the same input chirp voltage waveform and low-pass filter system as was used for measuring the transformers' responses. The distortions incorporated in the experiment results were calibrated out by removing the identified distortion responses. Therefore, the experimental results presented in this paper are free of measurement system introduced distortions. The calibration results of the 200 MΩ reference resistor measured by the FDS measurement circuit are illustrated in Figure 5.

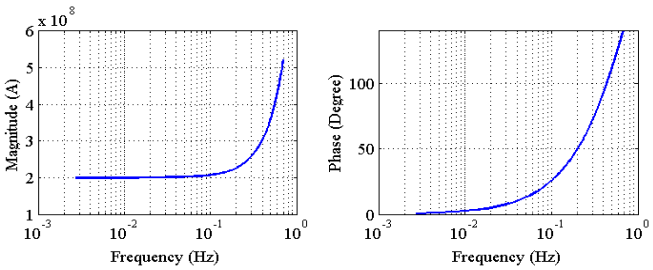

Figure 5. Spectrum of the 200 MΩ resistor

Figure 5 shows the distorted measured resistive spectrum due to the measurement chain. Any magnitude and phase distortions due to the measurement circuit can be eliminated using calibration.

4.2 EXPERIMENTAL SETUP

1) Single-phase Transformer

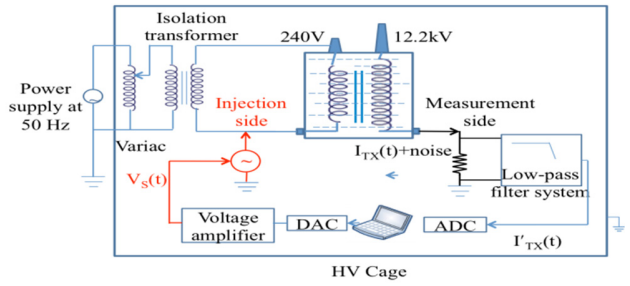

Figure 6. Laboratory arrangement of the Proposed FDS measurement on T1 and T2 in the high voltage cage.

The proposed FDS measurement arrangement for single-phase transformers under investigations is shown in Figure 6. The chirp waveform is generated using the 'Chirp' command in MATLAB installed in the laptop and the chirp signal voltage excitation is generated via Data Acquisition toolbox and a Digital Analog Converter (DAC) connected to a voltage amplifier. On the measurement side, the corresponding response current $I_{TX}(t)$ is passed through the analog low-pass filters to be amplified to give the filtered response current $I'_{TX}(t)$ which is then recorded through the Analog Digital Converter (ADC) and post-processed by the chirp-matched filter. The chirp swept time was set to 10^4 seconds for a 10^{-3} Hz to 10^0 Hz sweep.

The transformers under test were powered from the 50 Hz 240V mains supply via a Variac and an isolation transformer as illustrated in Figure 6. This results in 240 V on secondary winding and 12.2kV on primary winding.

2) Three-Phase Transformer Setup

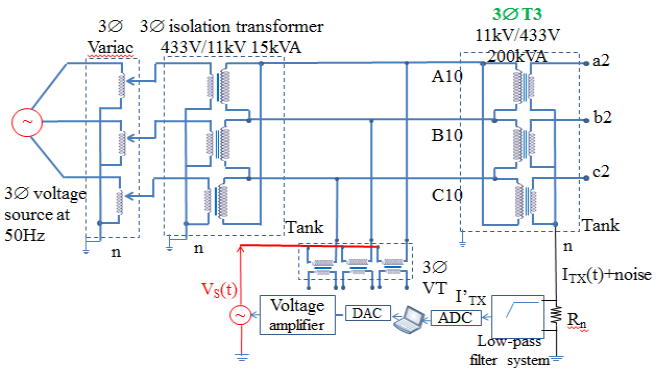

Figure 7. The circuit connections of the proposed method on T3.

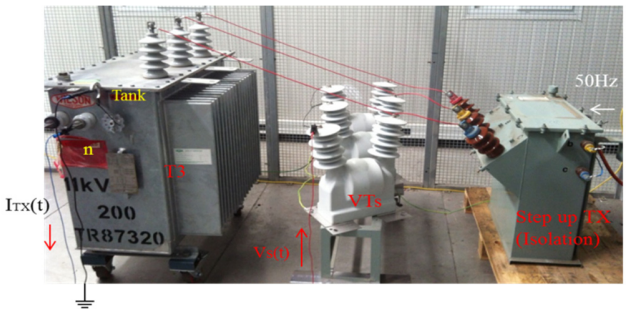

Figure 8. Physical connections of T3 in the high voltage cage

The winding configuration of the 3-phase transformer T3 under test is a Delta-Wye connection. According to the method mentioned before, the $V_S(t)$ injection point is created through the VTs' neutral on the primary side (Delta-connected) and the dielectric current response $I_{TX}(t)$ is measured through the neutral resistor on the secondary side (Wye-connected), illustrated in Figure 7 and Figure 8. Similarly to the arrangement of the single-phase transformers tests, T3 was powered from the 50 Hz 433 V mains supply via a 3-phase Variac. The VTs chosen here were epoxy encapsulated VTs as their dielectric response was an extremely small within the low frequency band from 10^{-3} Hz to 10^0 Hz when compared to oil-paper insulation and can be neglected.

For the laboratory test, the isolation transformer, illustrated in Figure 6 and Figure 7 was to prevent the low frequency FDS

excitation signals from entering the mains and to make the experiments safe. The measurements were performed with the HV windings of the transformers under open circuited i.e. without load current. This is done to investigate the expected nonlinear dielectric phenomenon excited by high magnitude mains frequency electric field effects. Under loaded condition, power frequency current could flow through the neutral connections due to load imbalance. This current should be significantly rejected by the measurement chain low-pass filter.

4.3 PROPOSED MEASUREMENT CIRCUIT VERIFICATION

Importantly, the conventional offline FDS experiments were implemented by utilizing the exactly same measurement circuits designed for the proposed measurements in order to compare the results from conventional offline and energized cases in the same base. The conventional FDS results were verified with the simulated FDS results of T1, T2 and T3. The simulated results were calculated from the polarization as well as depolarization currents of the time domain PDC measurements implemented by authors on the three transformers according to the method in [7].

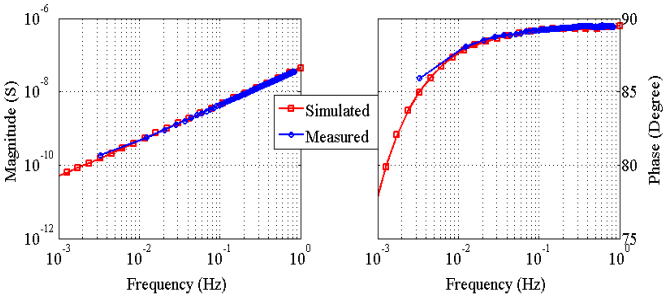

Figure 9. Simulated and Measured admittance response of T3.

Figure 9 illustrates the comparisons between the measured and simulated responses of the insulation admittance of T3. The comparisons of T1 and T2 have the similar results. Here, the value of coefficient of determination R^2 for magnitude deviation is not less than 0.99 while the value for phase deviation is not less than 0.89. These good fits between the measured and simulated responses are adequate to verify the feasibility and validity of the proposed FDS measuring circuit system.

4.4 MEASUREMENT RESULTS

Figure 10 shows the time domain responses of T1 obtained from the energized experiments. The response current $I'_{TX}(t)$ is evidently corrupted by noise from the measurement circuits as well as the attenuation effects from the low-pass filter system. The similar results were obtained from T2 and T3 as well. These time domain responses were further processed by using the chirp-matched filter to extract the magnitude and phase information in the frequency domain. The associated distortions from both filter system and chirp-matched filter were further removed by the calibration method mentioned in section 4.1.

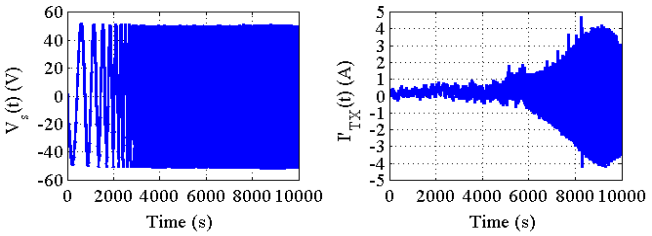

Figure 10. Chirp voltage excitation and its response current from the filter system.

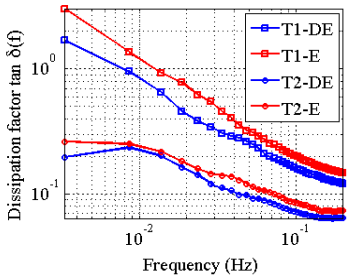

Figure 11. Comparison between energized and de-energized dissipation factor (DE: de-energized; E: energized).

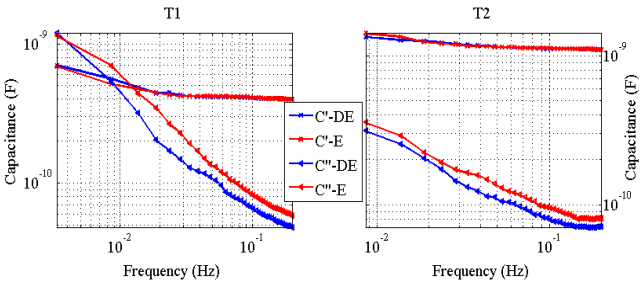

Figure 12. Comparison between energized and de-energized complex capacitance responses (C′: real part of capacitance; C″: imaginary part of capacitance) (DE: de-energized; E: energized).

Figure 11 illustrates and compares the energized dissipation factor responses of T1 and T2. It shows that the overall condition of the insulation system of T1 is more deteriorated compared with the status of T2. However, a small deviation appears when the energized and de-energized responses are compared with each other. In previous works in [24], the relatively small differences were found related to the imaginary part of capacitance C″, as illustrated in Figure 12, which are associated with total resistive losses. The nonlinear phenomenon expected in the energized condition is due to the combination of mains frequency with the low frequency electrical field.

For the 3-phase transformer T3, the dielectric responses results extracted from the energized and de-energized setups are compared in Figure 13. Here, the canyon in the loss results in the figure is due to noise in the system and is acceptable. The temperature rise during the experiments was negligible under the no load condition. On the basis of the comparisons, the two plots illustrate that no discernable differences are observed in comparison to the single-phase transformer cases. A reason for this dissimilarity is that the transformer T3 insulation system is free of dipoles and contaminants and the losses are too slight to make any significant differences since

the transformer is new and not been used before. The unaged insulation system behaves like an ideal capacitor. Therefore, the nonlinear phenomenon as seen in the energized results from T1 and T2 could not be significantly observed in energized results of T3, due to the relatively good condition of the insulation system of T3.

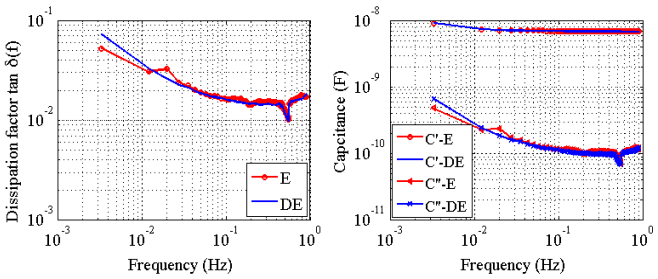

Figure 13. Comparison between de-energized and energized responses of T3 (C': real part of capacitance; C'': imaginary part of capacitance) (DE: de-energized; E: energized).

4.5 NONLINEAR DIELECTRIC RESPONSE

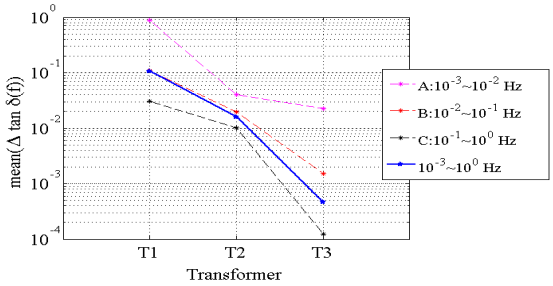

Figure 14. Mean difference values between energized and de-energized dissipation factor responses.

To evaluate the nonlinearity effects based on the above FDS measurements, the averaged difference values between energized and de-energized dissipation factor responses of the three transformers under test are calculated. The values are computed according to equation (8). The results are plotted in Figure 14. The dashed curves for A, B and C represent the mean ($\Delta\tan\delta$) values distributed in the three frequency bands (A: $10^{-3} - 10^{-2}$ Hz; B: $10^{-2} - 10^{-1}$ Hz; C: $10^{-1} - 10^{0}$ Hz;) whilst the solid blue line presents the values calculated from the whole frequency band.

$$\text{mean}(\Delta\tan\delta) = \frac{\sum_{k=1}^{N_S} |\tan_E\delta(f_k) - \tan_{DE}\delta(f_k)|}{N_S} \quad (8)$$

where N_S denotes the uniformly interpolated sample number in each response; $\tan_E(f_k)$ and $\tan_{DE}(f_k)$ represent energized and de-energized responses, respectively.

In Figure 14, the descending trends of the mean($\Delta\tan\delta$) values calculated from the three frequency bands are consistent with the whole band averaged value illustrated by the solid blue line. Therefore, the level of the nonlinearity phenomenon can be reflected and represented by this single curve that represents the general relationship between nonlinearity and insulation degradation condition. It is clear that the nonlinear phenomenon tends to increase as the insulation system of the transformer under test becomes impaired and this is more evident at low frequencies.

Taking the phenomena of the above transformers into consideration, it is safe to conclude that the difference between energized and de-energized responses is mainly due to nonlinear phenomenon excited by the high magnitude electric field stress at rated mains voltage. A loss increment is observable if the insulation system under test is degraded. This conclusion implies that not only the operating temperature but also the power frequency stress has an effect on the dielectric response when the measurement is considered in a real-time online mode. Note also that the degree of nonlinearity is related to the degradation level of the insulation system under test.

5 CONCLUSION

Enhancements to the existing FDS measurement technique are proposed and successfully implemented on energized transformers with the view to developing an online diagnostic tool using neutral connections as the injection and measurement paths. If a neutral point is not available, it is possible to create a virtual neutral using the appropriate connection of single phase voltage measurement transformers. Analog and digital filtering is effectively used to remove unwanted noises and power frequency interfering signals from the measurements. A logarithmic chirp waveform excitation was used in measurements to reduce the measuring time with acceptable resolution in the frequency domain.

A low frequency nonlinear phenomenon was observed when conducting measurements under energized conditions. This nonlinear response is attributed to the resistive losses excited by the combination of the high-level power frequency and the low frequency electrical fields [16]. Further, the degree of this nonlinearity is related to the deterioration level of the oil-paper insulation system under test since the resistive losses tend to rise as the insulation system degrades. However, more study will be required in the future to investigate the correlation between the presence of the high-level power frequency electric field and the mechanism of the nonlinearity.

The measurement design and the results obtained so far can be seen as the first step towards the development of an online diagnostic tool for dielectric measurements in the real world. In future work, practical techniques are required to isolate the dielectric response current in the neutral-to-earth path from all the other interfering noise sources that are present in the field. To effectively investigate the dielectric response of moisture in cellulose, improvements to the measuring system need to be made to lower the dielectric response frequencies below 10^{-3} Hz. Experimental work on loaded transformers is recommended to investigate the temperature effects corresponding to load variations on dielectric responses. In this case, the dielectric phenomenon under more realistic circumstances can be further studied.

ACKNOWLEDGMENT

This paper was developed within the CRC for Infrastructure and Engineering Asset Management, established and supported under the Australian Government's Cooperative Research Centres Program. The authors gratefully acknowledge the financial support provided by the CRC.

REFERENCES

[1] L. Ruijin, H. Jian, G. Chen, and Y. Lijun, "Quantitative analysis of ageing condition of oil-paper insulation by frequency domain spectroscopy," IEEE Trans. Dielectr. Electr. Insul., Vol. 19, pp. 821-830, 2012.

[2] J. Blennow, C. Ekanayake, K. Walczak, B. Garcia, and S. M. Gubanski, "Field experiences with measurements of dielectric response in frequency domain for power transformer diagnostics," IEEE Trans. Power Del., Vol. 21, pp. 681-688, 2006.

[3] T. K. Saha, "Review of modern diagnostic techniques for assessing insulation condition in aged transformers," IEEE Trans. Dielectr. Electr. Insul., Vol. 10, pp. 903-917, 2003.

[4] W. S. Zaengl, "Dielectric spectroscopy in time and frequency domain for HV power equipment. I. Theoretical considerations," IEEE Electr. Insul. Mag., Vol. 19, No. 5, pp. 5-19, 2003.

[5] T. K. Saha, "Review of modern diagnostic techniques for assessing insulation condition in aged transformers," IEEE Trans. Dielectr. Electr. Insul, Col. 10, pp. 903-917, 2003.

[6] S. Birlasekaran and X. Yu, "Relaxation studies on power equipment," IEEE Trans. Dielectr. Electr. Insul., Vol. 10, pp. 1061-1077, 2003.

[7] T. K. Saha, P. Purkait, and F. Muller, "Deriving an equivalent circuit of transformers insulation for understanding the dielectric response measurements," IEEE Trans. Power Del., Vol. 20, pp. 149-157, 2005.

[8] J. Hao, R. Liao, G. Chen, Z. Ma, and L. Yang, "Quantitative analysis ageing status of natural ester-paper insulation and mineral oil-paper insulation by polarization/depolarization current," IEEE Trans. Dielectr. Electr. Insul., Vol. 19, pp. 188-199, 2012.

[9] M. Koch and T. Prevost, "Analysis of dielectric response measurements for condition assessment of oil-paper transformer insulation," IEEE Trans. Dielectr. Electr. Insul., Vol. 19, pp. 1908-1915, 2012.

[10] A. K. Pradhan, B. Chatterjee, and S. Chakravorti, "Effect of temperature on frequency dependent dielectric parameters of oil-paper insulation under non-sinusoidal excitation," IEEE Trans. Dielectr. Electr. Insul., Vol. 21, pp. 653-661, 2014.

[11] J. Obrzut and K. Kano, "Impedance and nonlinear dielectric testing at high AC voltages using waveforms," IEEE Trans. Instrum. Meas., Vol. 54, pp. 1570-1574, 2005.

[12] A.K.Jonscher, *Dielectric Relaxation in Solids,* London: Chelsea Dielectrics Press, 1983.

[13] M. Koch, M. Krueger, and S. Tenbohlen, "On-site methods for reliable moisture determination in power transformers," in IEEE Power and Energy Soc., Transmission and Distribution Conf. and Exposition, pp. 1-6, 2010.

[14] A. Setayeshmehr, I. Fofana, C. Eichler, A. Akbari, H. Borsi, and E. Gockenbach, "Dielectric spectroscopic measurements on transformer oil-paper insulation under controlled laboratory conditions," IEEE Trans. Dielectr. Electr. Insul., Vol. 15, pp. 1100-1111, 2008.

[15] X. Qi, Z. Zheng, and S. Boggs, "Engineering with nonlinear dielectrics," IEEE Electr. Insul. Mag., Vol. 20, No. 6, pp. 27-34, 2004.

[16] C. Ekanayake, S. M. Gubanski, A. Graczkowski, and K. Walczak, "Frequency response of oil impregnated pressboard and paper samples for estimating moisture in transformer insulation," IEEE Trans. Power Del., Vol. 21, pp. 1309-1317, 2006.

[17] T. W. Dakin, "Conduction and polarization mechanisms and trends in dielectric," IEEE Trans. Electr. Insul. Mag., Vol. 22, No. 5, pp. 11-28, 2006.

[18] M. Koch, M. Kruger, and M. Gupta, "A fast and reliable dielectric diagnostic method to determine moisture in power transformers," in Int'l Sympos. Electrical Insulating Materials (ISEIM), pp. 672-672, 2008.

[19] M. Jaya, D. Geissler, and T. Leibfried, "Accelerating Dielectric Response Measurements on Power Transformers-Part I: A Frequency-Domain Approach," IEEE Trans. Power Del., Vol. 28, pp. 1469-1473, 2013.

[20] S. W. Smith, *Digital Signal Processing: a Practical Guide for Engineers and Scientists*, Amsterdam; Boston: Newnes, 2003.

[21] B. Sonerud, T. Bengtsson, J. Blennow and S. M. Gubanski, "Dielectric Response Measurements Utilizing Semi-Square Voltage Waveforms," IEEE Trans. Dielectr. Electr. Insul., Vol. 15, pp. 920-926, 2008.

[22] M. Bagheri, M. S. Naderi, and T. Blackburn, "Advanced transformer winding deformation diagnosis: moving from off-line to on-line," IEEE Trans. Dielectr. Electr. Insul., Vol. 19, pp. 1860-1870, 2012.

[23] T. De Rybel, A. Singh, J. A. Vandermaar, M. Wang, J. R. Marti, and K. D. Srivastava, "Apparatus for Online Power Transformer Winding Monitoring Using Bushing Tap Injection," IEEE Trans. Power Del., Vol. 24, pp. 996-1003, 2009.

[24] X. Yang, S. Nielsen, and G. Ledwich, "Investigations of dielectric monitoring on an energised transformer oil–paper insulation system," IET Sci., Measur. Techn., Vol. 9, pp. 102-112, 2015.

[25] A. H. Etemadi and A. Rezaei-Zare, "Optimal Placement of GIC Blocking Devices for Geomagnetic Disturbance Mitigation," IEEE Trans. Power Syst., Vol. 29, pp. 1-10, 2014.

Xu Yang received her Ph.D. degree from Queensland University of Technology (QUT), Brisbane, Australia in 2015. She is now working as an engineer in Maintenance & Test Center of China Southern Power Grid Extra High Voltage Power Transmission Company. Her research interests are online condition monitoring on power transformers, high voltage measurements.

Shawn Nielsen obtained his Ph.D. from the University of the Witwatersrand, South Africa in 2002. He joined QUT as a Senior Research Fellow working on transformer condition monitoring. Shawn's fields of interests include gas breakdown, partial discharge, high voltage measurements, electric field modelling and the effect of Geomagnetically Induced Currents (GIC's) on power networks.

Gerard Ledwich (M'73-SM'92) received the Ph.D. degree in electrical engineering from the University of Newcastle, Australia, in 1976. He has been Chair Professor in Power Engineering at Queensland University of Technology, Brisbane, Australia, since 2000. His interests are in the areas of online condition monitoring of oil-paper insulation, power systems, power electronics, and controls. He is a Fellow of I.E. Australia.